Chapter 3

Zinc(II) complexes with thiophene-containing ligands

3.1 Introduction

Complexes of zinc with sulfur ligands have been studied widely because of their biological importance and their use as accelerators in the vulcanization of rubber[1]. In addition, the model compound, $[Zn(S_2CPh)_2]$ and its derivatives are of interest in material science.

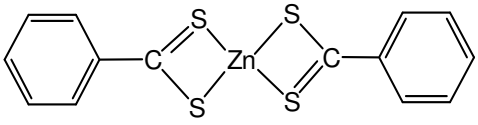

Figure 3.1 Tetrahedral $[Zn(S_2CPh)_2]$

Bonamico[2] suggested that, with the addition of p-alkyl or p-alkyloxy chains to the phenyl rings of $[Zn(S_2CPh)_2]$, rod-like molecules should result. In 1988 Adams *et al*.[3] synthesized the alkyloxy dithiobenzoate complexes of zinc, nickel and palladium and reported on their mesomorphic properties. Octyloxy dithiobenzoate complexes of zinc showed a nematic phase, while the nickel and the palladium analogues showed both nematic and smectic phases. X-ray determinations of single red crystals of octyloxy dithiobenzoate complexes of zinc showed that the molecules were dimeric, containing 8-membered $Zn_2S_4C_2$ rings, formed by the fusion of two ZnS_2C rings, and in which the geometry about zinc approximated to trigonal bipyramidal[4]. It was reported that EXAFS data for the octyloxy complex of zinc clearly indicated that the same structures are in the nematic mesophase as

in the red crystals. Thus the molecules are not tetrahedral about the metal, and the dimeric structure persists into the mesophase. It has already been noted that mesomorphism in metallomesogens seems to be incompatible with a tetrahedral geometry about the central metal[5].

Since 1985 many metallomesogens of zinc have been made with different ligands, monodentate (4-substituted pyridines)[5,6], bidentate (β-diketonates, dithiolenes, carboxylates, cyclometalated aromatic amines)[3-5,7], or polydentate (phthalocyanines[8-10], porphyrins[11,12]) and the mesomorphism of these complexes were examined. Some of the zinc complexes were not mesomorphic. Hoshino[13] ascribed the fact that the zinc analogues of the mesomorphic copper salicylaldimines were not liquid crystalline to the complexes being tetrahedral. A very important group of zinc complexes displaying liquid crystal properties is those with nitrogen donor atoms. These contain flat, macrocyclic rings acting as tetradentate ligands and two classes of importance are substituted porphyrins (Figure 3.2) and phthalocyanines (Figure 3.3). Bruce[12] reported calamitic liquid crystal phases for zinc(II) complexes of 5,15-disubstituted porphyrins.

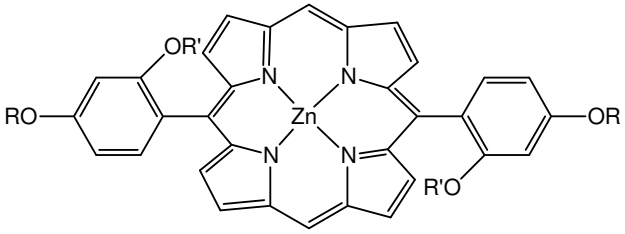

R = C_nH_{2n+1}, n = 8, 10, 12, 14, 16 (**A**); R = OR, R' = $S(O)_2C_6H_4$-p-NO_2(**B**)

Figure 3.2 Zinc complexes with porphyrin (**A**) and with lateral substituted (**B**) porphyrin ligands

The complexes showed smectic C phases, whereas uncoordinated porphyrins with their flat, disk-like geometries, normally display discotic phases[5]. In 1996 Wang and Bruce[14] showed that inherently disc-like porphyrins can be modified to be rod-like crystals with low melting points. This is achieved by using lateral substituents to prevent intermolecular π-π interactions. The thermal behaviour was investigated and it formed a nematic phase. The lateral group used was ortho-(para-nitrophenylsulphonyl)oxy group due to its strong electron-accepting ability.

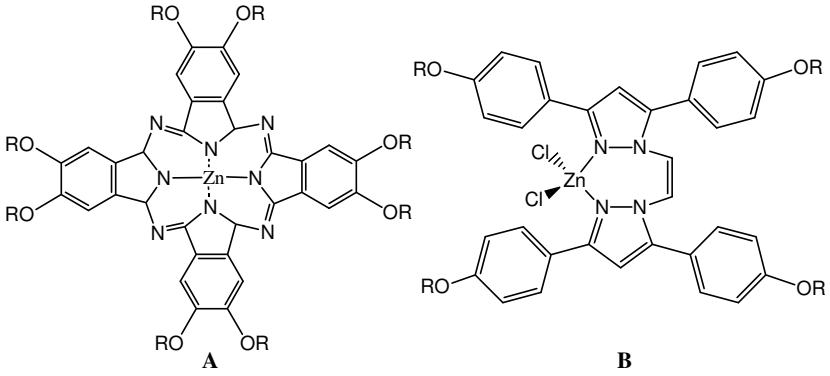

Figure 3.3 Zinc complexes with phthalocyanine (**A**) and pyrazolyl ligands (**B**)

Severs and co-workers[9] described the thermal behaviour of zinc phthalocyanines with eight peripheral dodecyloxy chains. Binnemans[10] reported the influence of the nature of the central metal ion on the transition temperatures of metal phthalocyanines with eight peripheral alkoxy chains. The melting points depended on the identity of the central metal ion and followed the order Ni(II) < (Cu(II) ≈ Co(II) < Zn(II) for increasing melting temperatures. Longer alkyloxy chains tend to lower the transition temperatures of the compounds. The melting points of these phthalocyanine complexes are in general higher than those of the corresponding metal-free phthalocyanines.

In the liquid crystalline zinc complexes described earlier, the geometry of the metal centre is either planar or trigonal bipyramidal[4-7]. Recently mesomorphism for zinc complexes have been reported regardless of the geometry (including tetrahedral) around the metal ion, with bis[3,5-bis(p-decyloxyphenyl)pyrazolyl]ethane[15] and hexacatenar 4,4'-disubstituted 2,2'-bipyridines[16] as ligands. Gimenez and coworkers[15] employed the idea of Date[17] that the controlled supramolecular assemblies possible with metal complexes can be obtained from suitable ligand design. The zinc complexes displayed enantiotropic smectic C and A phases. The molecular structure indicated that the zinc atom was in a tetrahedral environment of ligands, but the planes containing the pyrazole rings were arranged at angles of only 16^{o}, resulting in a macrostructure consisting of more or less planar layers.

In this study 5-alkyl-2-thiophenedithiocarboxylate complexes of zinc(II), analogues to the nickel(II) complexes described in chapter 2, were prepared and studied. Again small differences in structural features and electronic properties of the zinc complexes created by replacing a bridging phenyl by a thiophene unit were the main focus point. It was found that the presence of thiophene units helped to clear some of the confusion and irregularities in literature regarding the composition of nickel dithiocarboxylate complexes. Zinc dithiocarboxylate complexes were selected because of their close relationship with the metals Ni(II) and Cu(II) in their formation of stable complexes with S-donor ligands[3]. Zn(II) belongs to the d^{10}-configuration and affords, unlike Ni(II) (d^{8}) complexes, no

crystal field stabilization. The stability and the stereochemistry of a particular compound depends on the size and polarizing power of the Zn(II) cation and the steric requirements of the ligands.

3.2 Results and discussion

3.2.1 Synthesis and characterization

Five complexes of the type $[Zn(S_2CTR)_2]$ (where T =2,5-disubstituted thiophene unit, R = alkyl group; C_4H_9(**7**), C_6H_{13}(**8**), C_8H_{17}(**9**), $C_{12}H_{25}$,(**10**), $C_{16}H_{33}$(**11**)) were synthesized via a four-step reaction as shown in Scheme 3.1

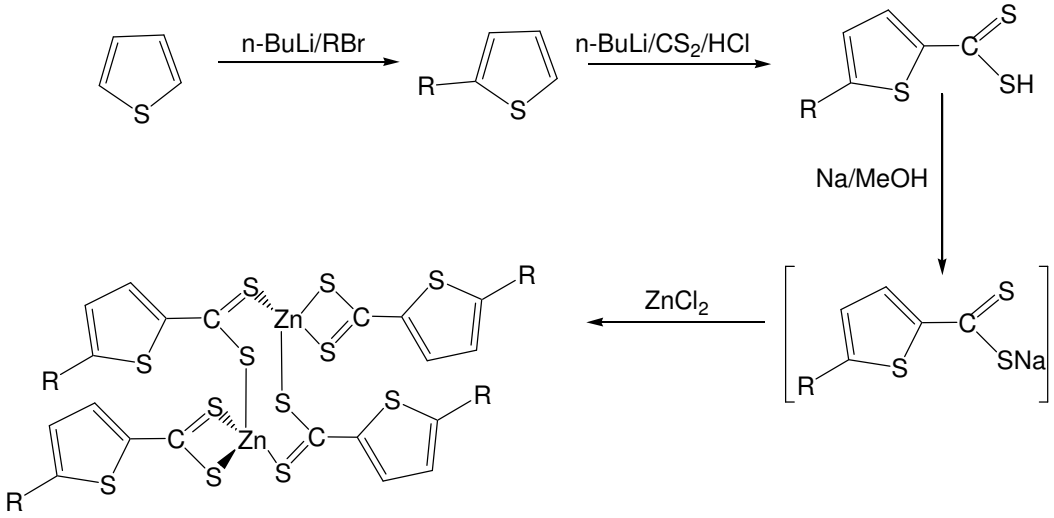

Scheme 3.1

The first three steps are similar to those described in chapter 2 for nickel(II) complexes. The sodium 5-alkyl-2-thiophenedithiocarboxylate compounds were synthesized according to literature procedures[18] as shown in Scheme 3.1. The first step involved the lithiation of thiophene at position 2 followed by the subsequent addition of alkyl bromide. In the second step, 2-alkyl thiophene was converted

into 5-alkyl-2-thiophenedithiocarboxylic acid. The first part of the reaction was done under an inert atmosphere. It involved the lithiation of alkyl thiophene at position 5 followed by the addition of CS_2. A deep red colour was observed on addition of CS_2. On further acidification with dilute hydrochloric acid, 5-alkyl-2-thiophenedithiocarboxylic acid was formed. Subsequently it was converted into the sodium salt by reacting with sodium methoxide.

The final step was similar to that used by Adams *et al.*[4] for the preparation of the corresponding dithiobenzoate complexes. On addition of a colourless solution of zinc chloride in water to a stirred solution of sodium 5-alkyl-2-thiophenedithiocarboxylate in water, the colour turned orange-brown and the reaction was allowed to stir for 3 hours at room temperature to ensure a complete reaction. The product was precipitated by adding excess methanol, separated by filtration and dried. Further purification was done on a silica gel column and the product was eluted with a mixture of hexane/dichloromethane (1:1) as eluent. IR and NMR spectroscopy were used to characterize the complexes. A structure determination (vide infra) revealed that two $[Zn(S_2CTR)_2]$ fused to afford a dizinc complex $[Zn_2(\mu\text{-}S_2CTR)_2(S_2CTR)_2]$.

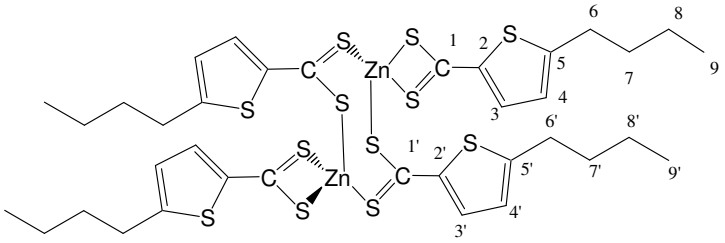

Figure 3.4

The carbon atoms are numbered starting with the carbon of CS_2 being C1 and numbering the hydrogen atoms with the same number as the carbons to which

they are attached. The bridging dithiocarboxylate ligands are numbered similarly but the atoms are indicated by adding apostrophes to the numbers.

The ^{1}H NMR spectrum of $[Zn_2(S_2CTC_4H_9)_4]$, **7** (Figure 3.5) displayed two doublets, at 7.87 ppm and 6.83 ppm in the arene region of the spectrum. The doublet signal at 7.87 ppm is assigned to H3 because it is closer to the dithiocarboxylate carbon (C1). The doublet signal at 6.83 ppm was assigned to H4 which is closer to the side of the alkyl (butyl) chain. The two doublets, which integrated for four hydrogen atoms, are indicative of two thiophene rings in a similar electronic environment. Hence, the terminal and bridging resonances in the ^{1}H NMR spectra coincides.

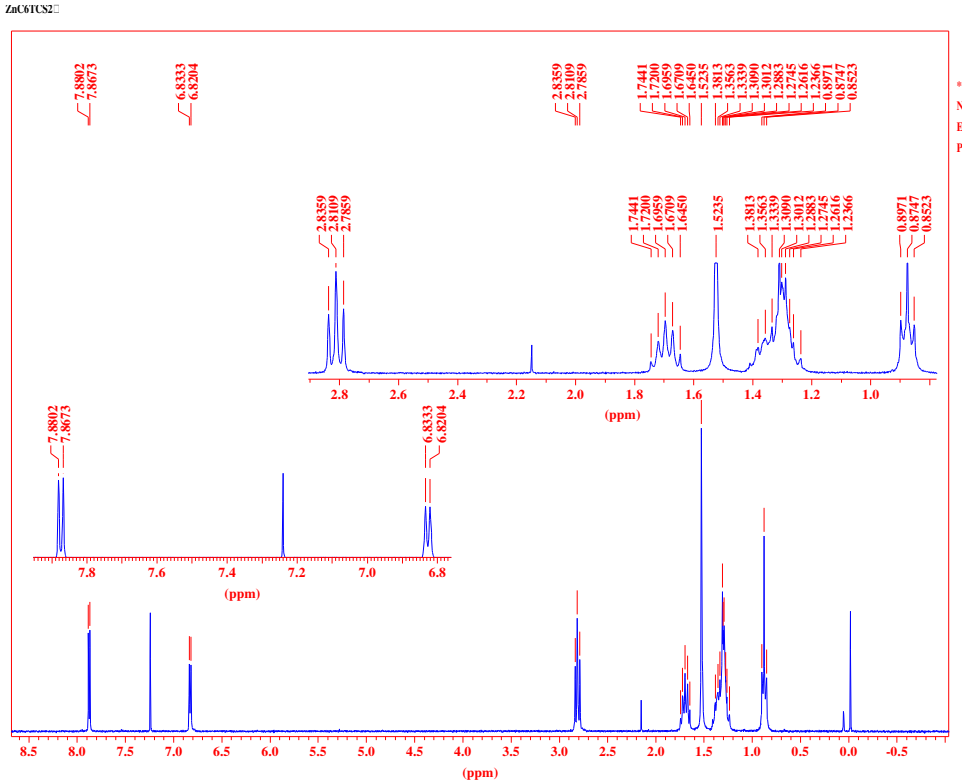

Figure 3.5 The ^{1}H NMR spectrum of $[Zn_2(S_2CTC_4H_9)_4]$ **7**

The signal at 2.82 ppm is assigned to the four protons of the two CH_2-groups attached to the two symmetrical thiophene rings. The multiplets at 1.66 and 1.42 ppm integrated for eight protons and represent the two middle CH_2-groups of the two butyl chains. The signal at 0.92 ppm integrated for six protons and was assigned to the two CH_3-groups at the end of the chains. The ^1H NMR spectra of all the complexes showed only two doublets in the arene region. The spontaneous insertion of a sulfur atom into the RCS_2-ligand in THF to give perthiocarboxylate ligands for the nickel(II) complexes was absent in the analogous zinc(II) complexes. However, similar insertions have been observed for zinc(II) benzenedithiocarboxylate complexes. The presence of the perthiocarboxylate ligands for nickel(II) complexes and absence thereof for zinc(II) complexes are ascribed to the electronic effects of the thiophene rings.

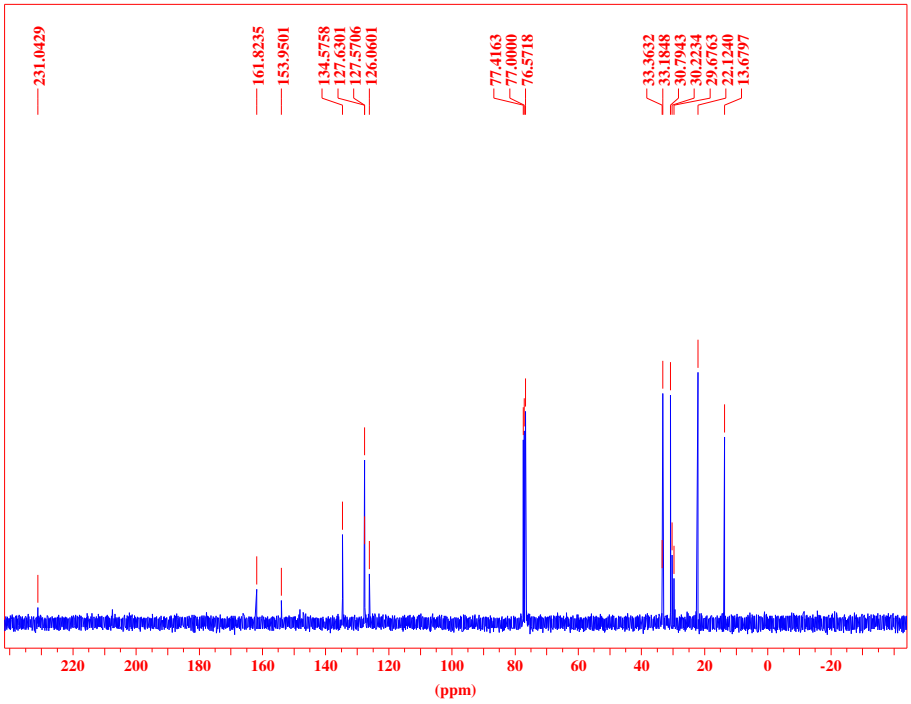

Figure 3.6 The ^{13}C NMR spectrum of $[Zn_2(S_2CTC_4H_9)_4]$ **7**

The ^{13}C NMR spectrum of $[Zn_2(S_2CTC_4H_9)_4]$, **7** (Figure 3.6) showed all the carbons of the thiophene rings, the butyl chains as well as that of the CS_2 chelate (C1). Again, no duplication of signals was observed, supporting the ^1H NMR data. None of the FAB mass spectra of any of the complexes gave a molecular ion peak or m/z-values assignable to fragment ions. The infrared spectra of all the complexes showed similar peaks. The infrared spectrum of $[Zn_2(S_2CTC_4H_9)_4]$, **7** showed prominent peaks at 2921, 1461, 1375, 1046, 980 and 721 cm^{-1}. The signal at 2921 cm^{-1} was assigned for the CH_2-groups of the alkyl chain and the peak at 1461 cm^{-1} was assigned for the arene-carbon (C-C thiophene) stretching frequency. The peak at 1375 cm^{-1} was assigned for the terminal CH_3 group. The peaks at 1046 and 980 cm^{-1} were assigned for C-S stretching frequencies of the dithiocarboxylate group. Usually the stretching frequencies of dithiocarboxylate complexes[19,20] are observed between 900 and 1100 cm^{-1}. The peak at 721 cm^{-1} was assigned for the arene C-H (thiophene). The infrared spectral values of **7-11** are given in Table 3.1.

Table 3.1 Spectral data of complexes **7-11**

Complex	^1H NMR (δ/ppm in $CDCl_3$)	^{13}C NMR (δ/ppm in $CDCl_3$)	IR (ν/cm^{-1} in Nujol)
$[Zn_2(S_2CTC_4H_9)_4]$ **7**	7.87 (d, 2H, H3, J=3.9), 6.83 (d, 2H, H4, J=3.6), 2.82 (t, 4H, H6, J=7.5), 1.66 (m, 4H, H7), 1.42 (m, 4H, H8), 0.92 (t, 6H, H9, J=7.2/7.5)	231.0 (C1), 161.8 (C2), 153.9 (C5), 134.6 (C3), 127.5 (C4), 33.2, 29.8, 22.1, 13.7 (C6-C9)	2921 (vs), 1461 (vs), 1375 (s), 1046 (m), 980 (m), 721 (s)
$[Zn_2(S_2CTC_6H_{13})_4]$ **8**	7.87 (d, 2H, H3, J=3.9), 6.83 (d, 2H, H4, J=3.9), 2.81 (t, 4H, H6, J=7.5), 1.69	207.0 (C1), 162.5 (C2), 148.7 (C5), 135.2 (C3), 128.0 (C4), 31.8, 31.5,	2921 (vs), 1458 (vs), 1375 (s), 1050 (m), 978

	(m, 4H, H7), 1.30 (m, 12H, H8-H10), 0.87 (t, 6H, H11, J=6.7)	31.4, 29.0, 22.9, 14.4 (C6-C11)	(m), 722 (s)
$[Zn_2(S_2CTC_8H_{17})_4]$ **9**	7.87 (d, 2H, H3, J=3.9), 6.82 (d, 2H, H4, J=3.9), 2.80 (t, 4H, H6, J=7.5/7.8), 1.69 (m, 4H, H7), 1.26 (m, 20H, H8-H12), 0.87 (t, 6H, H13, J=6.7/7.0)	207.5 (C1), 162.1 (C2), 148.3 (C5), 134.8 (C3), 127.6 (C4), 31.8, 31.1, 30.6, 29.2, 29.1, 29.0, 22.6, 14.0 (C6-C13)	2920 (vs), 1461 (vs), 1375 (s), 1048 (m), 970 (m), 721 (s)
$[Zn_2(S_2CTC_{12}H_{25})_4]$ **10**	7.85 (d, 2H, H3, J=3.9), 6.81 (d, 2H, H4, J=3.9), 2.79 (t, 4H, H6, J=7.5), 1.68 (m, 4H, H7), 1.23 (m, 36H, H8-H16), 0.85 (t, 6H, H17, J=6.2/7.0)	206.8 (C1), 161.6 (C2), 134.3 (C5), 128.8 (C3), 127.5 (C4), 35.7, 31.9, 31.1, 30.9, 29.7, 29.6, 29.4, 29.2, 29.0, 26.4, 22.7, 14.1 (C6-C17)	2921 (vs), 1460 (vs), 1375 (s), 1046 (m), 981 (m), 720 (s)
$[Zn_2(S_2CTC_{16}H_{33})_4]$ **11**	7.86 (d, 2H, H3, J=3.9), 6.82 (d, 2H, H4, J=4.1), 2.80 (t, 4H, H6, J=7.5), 1.67 (m, 4H, H7), 1.24 (m, 52H, H8-H20), 0.86 (t, 6H, H21, J=6.5/6.7)	207.4 (C1), 161.5 (C2), 153.9 (C5), 134.2 (C3), 127.5 (C4), 31.9, 31.3, 31.1, 30.8, 30.7, 30.5, 29.8, 29.7, 29.6, 29.5, 29.3, 29.2, 29.0, 26.4, 22.7, 14.1 (C6-C21)	2921 (vs), 1461 (vs), 1375 (s), 1049 (m), 977 (m), 721 (s)

The ^{1}H and ^{13}C NMR data of the complexes suggest that the complexes are either monomers or the chemical shifts of the terminal and bridging dithiocarboxylate ligands are the same in solution.

3.2.2 Molecular structure of $[Zn_2(S_2CTC_6H_{13})_4]$ (**8**)

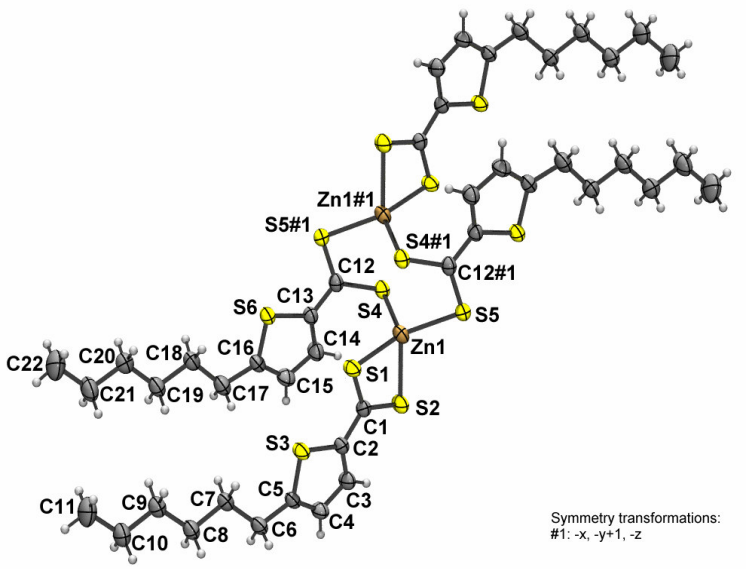

Figure 3.7 An ORTEP[21]+ POV-Ray[22] plot of the geometry of **8**

The molecular structure of **8** was determined by single crystal X-ray crystallography. Single crystals suitable for crystal structural determination were obtained by slow diffusion of hexane into a CH_2Cl_2 solution of **8** at room temperature. An ORTEP + POV-Ray plot of the geometry of **8** in Figure 3.7 and a computer generated model of **8** in figure 3.8 are given. Selected bond lengths are given in Table 3.2 and selected bond angles in Table 3.3.

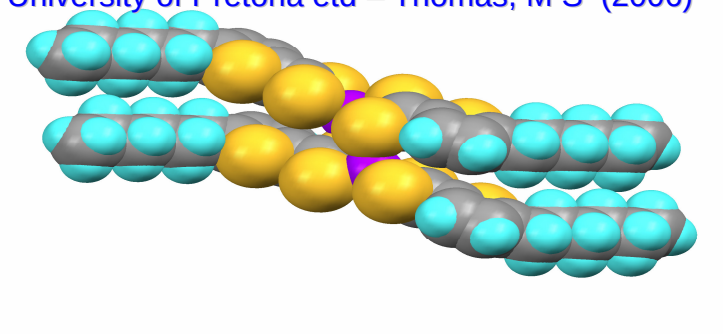

Figure 3.8 A computer generated model of **8**

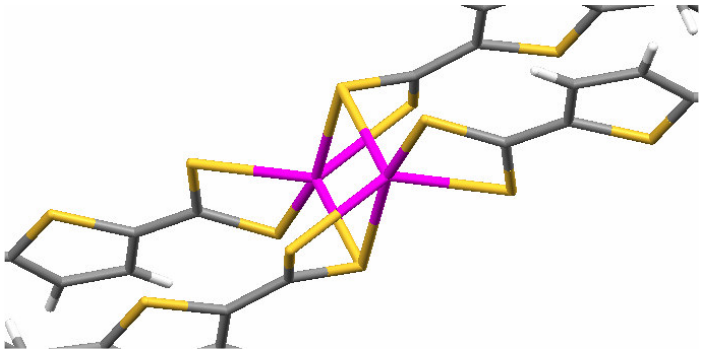

Figure 3.9 View of molecule showing the distorted trigonal bipyramidal arrangement of sulfur atoms around the zinc atoms

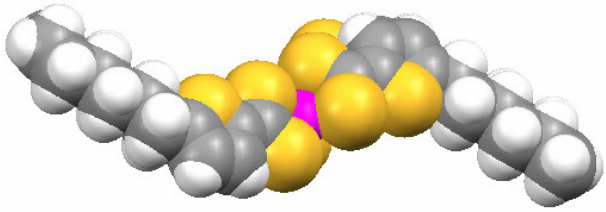

Figure 3.10 Side-on view showing the step-rod assembly of atoms as a result of the five-member thiophene rings

The structure of **8** can be compared to an analogous structure described for $[Zn_2(S_2CBC_8H_{17})_4]$ by Adams *et al.*[4]. Both structures display a dimeric assembly

with significant interaction between a sulfur of each monomer with the zinc metal of the other monomer in the solid state. As a result an eight-membered ring is formed with a chair conformation consisting of two zinc and two carbon atoms and four sulfur atoms. In the monomeric structure of $[Zn(S_2CPh)_2]^4$ or the dithiocarbamate $[Zn(S_2CNEt_2)_2]^4$ the zinc has a tetrahedral arrangement of ligands.

The molecular structure of **8** in the solid state is illustrated in Figure 3.7. Each molecule exists as a centrosymmetric dimer with the zinc atom in a five coordinated ligand environment with geometry that more closely resembles trigonal bipyramid (Figure 3.9). The dithiocarboxylate chelate ligands each bridge between an axial and an equatorial site with subtended angles of 67 or 75°. The remaining equatorial site is occupied by a sulfur already occupying an axial site of an adjacent, centrosymmetrically related, zinc co-ordination polyhedron. Four of the five zinc-sulfur bonds, excluding that to the axial bridging sulfur, S(4)#1, are short.

The distance between the zinc and axial bridging sulfur, S(4)#1, in structure **8** is 2.88Å, which is longer than the one reported for dithiobenzoate complexes, 2.83Å. The main difference between the overall shape of **8** compared to the linear structure of $[Zn_2(8\text{-odtb})_4]$ is the step-rod pattern that emerges for **8** in one plane whereas the p-benzene substituted octyloxy is linearly rod-shaped. This is a consequence of the five-member thiophene rings that cause a kink in the chains and can be seen in Figure 3.10. Figure 3.11 shows the packing of the lamellar rods and calamitic features.

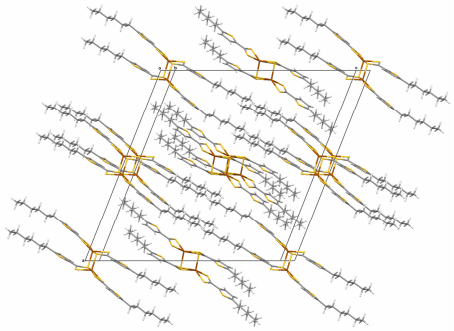

Figure 3.11 Shows the packing of the lamellar rods and calamitic features

Table 3.2 Selected bond lengths for **8**[a]

Atoms	Bond length (Å)	Atoms	Bond length (Å)
Zn(1)-S(4)#1	2.884(8)	[a]S(3)-C(2)	1.727(3)
Zn(1)-S(5)	2.354(8)	S(6)-C(16)	1.715(3)
Zn(1)-S(2)	2.454(8)	C(1)-C(2)	1.444(3)
Zn(1)-S(1)	2.369(7)	C(2)-C(3)	1.371(4)
Zn(1)-S(4)	2.392(8)	C(3)-C(4)	1.388(4)
S(1)-C(1)	1.701(3)	C(4)-C(5)	1.362(4)
S(2)-C(1)	1.690(3)	C(12)-C(13)	1.435(4)
S(4)-C(12)	1.723(3)	C(13)-C(14)	1.379(4)
S(5)-C(12)#1	1.683(3)	C(14)-C(15)	1.391(4)
S(3)-C(2)	1.727(3)	C(15)-C(16)	1.366(4)
S(6)-C(13)	1.729(3)	C(12)-S(5)#1	1.683(3)

[a] The corresponding bond lengths in thiophene are C(2)-S 1.714(1) Å, C(2)-C(3) 1.370(2) Å, C(3)-C(4) 1.423(2) Å[23]

Table 3.3 Selected bond angles for **8**

Atoms	Bond angle (°)	Atoms	Bond angle (°)
S(5)-Zn(1)-S(4)#1	67.62(2)	S(5)-Zn(1)-S(2)	111.59(3)
S(1)-Zn(1)-S(4)#1	96.96(3)	S(1)-Zn(1)-S(4)	117.86(3)
S(4)-Zn(1)-S(4)#1	82.43(3)	S(1)-Zn(1)-S(2)	74.74(3)
S(2)-Zn(1)-S(4)#1	167.72(3)	C(5)-S(3)-C(2)	92.31(13)
S(4)-Zn(1)-S(2)	109.35(3)	C(1)-S(1)-Zn(1)	83.99(9)
S(5)-Zn(1)-S(1)	134.47(3)	C(12)-S(4)-Zn(1)	98.94(9)
S(5)-Zn(1)-S(4)	102.78(3)	C(12)#1-S(5)-Zn(1)	93.72(9)

The bond lengths and bond angles of free thiophene[23] are compared with bond distances and angles of coordinated thiophene in **8**. The bond length of C-S increases slightly during coordination whereas the bond angle C(2)-S-C(5) remains the same. The bond length between carbon atoms on one side of the coordinated thiophene is smaller. In free thiophene the delocalization is within the ring whereas for **8** it is outwards towards the CS_2 ligand. This is manifested in the significantly shorter C(3)-C(4) bond distance in **8.** The distance of 1.44Å for C(1)-C(2) is shorter than the averaged distance for C-C (1.54Å) single bonds but longer than the averaged distance for C-C (1.34Å) double bonds. This may be due to the charge delocalization present in the thiophene ring in pi-contact with CS_2 and metal.

3.2.3 Thermal properties

The thermal properties of the complexes were preliminarily examined by Differential Scanning Calorimetry (DSC). The DSC thermogram reveals the presence of mesophases and liquid crystal phases by detecting the enthalpy change that is associated with a phase transition. Complexes **7**, **8** and **11** showed single sharp endothermic peaks whereas **9** and **10** showed two broad peaks, one small and one medium endothermic peak during melting. Ohta and coworkers[24] suggested that the double melting behaviour (two endothermic peaks) of long chain substituted compounds is a thermal behaviour close to mesomorphism. Figure 3.12 shows the DSC thermogram for $[Zn(S_2CTC_8H_{17})_2]$ **9**.

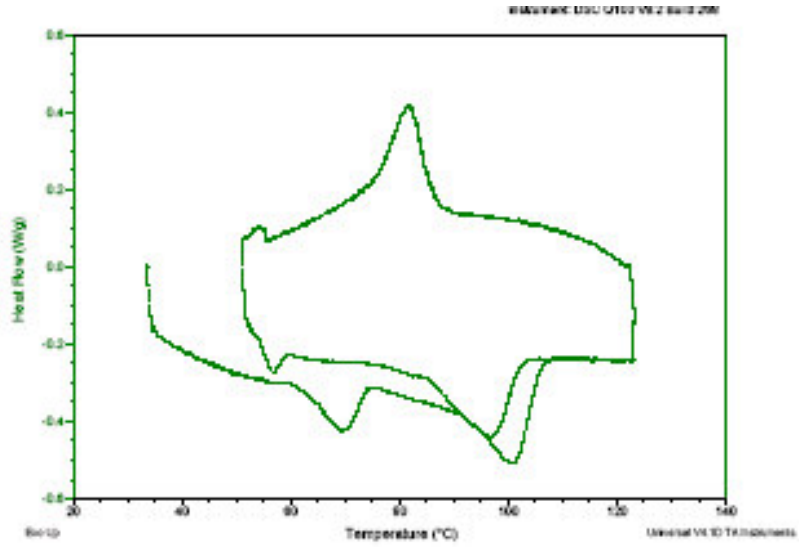

Figure 3.12DSC thermogram of **9**

Complex **9** showed two endothermic peaks, at 69°C and 102°C. The first peak at 69°C during the heating cycle is regarded as a crystal-crystal transition. The peak at 102°C is regarded as the melting point of the complex. Sometimes multiple endothermic events might represent transitions from one crystalline state to

another crystalline state, which occur when the substance exist in different molecular packing in the solid state at different temperatures[25]. Complex **10** also showed two endothermic peaks. The melting point peaks of **9** and **10** are broad whereas the melting point peaks of **7**, **8** and **11** are very sharp. The sharpness of the melting point gives an indication of the purity of the complex. Low molecular weight compounds with liquid crystalline properties are expected to have sharp melting points. The melting points of **7-11** from DSC are given in Table 3.4.

Table 3.4 Melting points of **7-11** complexes

Complex	Chain length	Melting point (^{o}C)
7	C_4H_9	132
8	C_6H_{13}	119
9	C_8H_{17}	102
10	$C_{12}H_{25}$	84
11	$C_{16}H_{33}$	52

The dependence of melting points of the complexes **7-11** on the chain length is depicted in Figure 3.13.

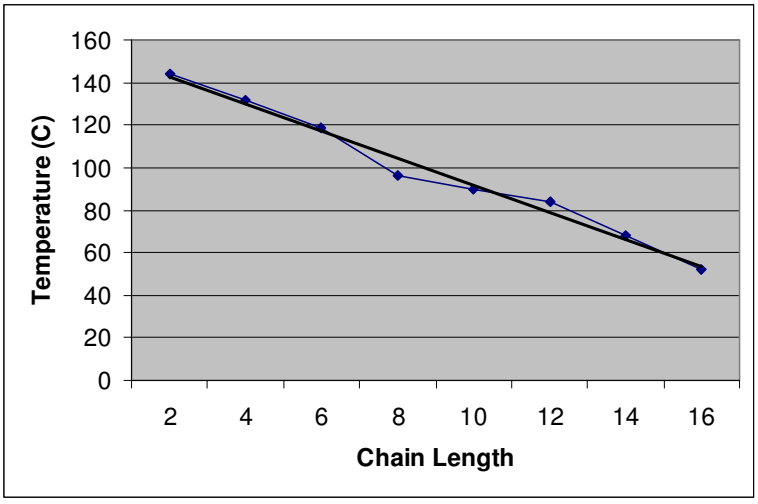

Figure 3.13 Dependence of the melting points of **7-11** on the chain length

The trend in the melting points is a steady decrease as the alkyl chain length of complexes increased (Figure 3.13). This trend was observed earlier for a homologous series of complexes that differ only in chain length[26]. The highest temperature 132°C for the shortest chain (C_4) and the lowest temperature 52°C for the longest chain (C_{16}) were observed. It is of interest to note that there is a linear decrease of melting points with increase in chain length. This has been ascribed to greater disorder caused by longer alkyl chains in the complexes.

Two complexes, one with sharp endothermic peak **11** and the other one **10** with two broad endothermic peaks were also examined by Hot-stage Polarising Optical microscopy. The complex **11** directly melted to the isotropic liquid without showing any mesophases. Complex **10**, when looking at the sample between crossed polarizers gave an impression that there is a mesophase present above 80°C. However, careful examination revealed that the birefringence observed was not due to a mesophase but due to tiny crystals floating in an isotropic melt. Cooling of the samples resulted in simple crystallization without forming any mesophases. Therefore complex **10** is not liquid crystalline.

3.3 Experimental

3.3.1 General

All commercially available chemicals were used as received. Solvents were dried and distilled under nitrogen prior to use. Thiophene was purified as described by Spies and Angelici[27]. All reactions were performed in an inert atmosphere of

either nitrogen or argon by using Schlenk techniques and vacuum-line. Column chromatography was carried out using silica gel.

Infrared spectra were recorded on a Perkin Elmer Spectrum 1000 FT-IR spectrophotometer. All NMR spectra were recorded in deuterated chloroform using the chloroform peak as standard on a Bruker ARX – 300 spectrometer.

Liquid-crystalline properties were examined on a Differential Scanning Calorimeter (DSC) Q 100 V8.2 Build 268 and Hot-stage Polarising Optical Microscope (POM) Olympus BX60 equipped with a Linkam THMS600 hot stage and a Linkam TMS93 Programmable temperature controller.

3.3.2 Structure determination of 8

A crystal of size 0.34 x 0.14 x 0.05 mm^3 was mounted in a sealed capillary tube for data collection. All geometric and intensity data were collected on a Siemens SMART diffractometer with a CCD detector.

3.3.3 Synthesis

All the complexes were synthesized via a four-step reaction in a similar manner. A typical procedure for complex **7** is described.

Preparation of 2-butyl thiophene

The procedure used is similar to the one described by Brandsma[18].The reaction was done in an inert atmosphere. n-Butyl lithium (15.6 ml, 25.0 mmol) was added to a mixture of THF (50.0 ml) and hexane (30.0 ml), which was cooled to -20^{o}C. Thiophene (1.68 g, 20.0 mmol) was introduced over 10 minutes with cooling

between 0°C and 10°C. The cooling bath was removed and allowed to rise to the room temperature. Butyl bromide (2.74 g, 20.0 mmol) was added in one portion without external cooling. The temperature of the solution was raised to 50°C and kept at this temperature for a further 30 minutes after which 100 ml of ice water was added with vigorous stirring. Two separate layers were observed and the separation was done in air. After separation of the layers, two extractions with diethyl ether were carried out. The combined organic solutions were dried over anhydrous $MgSO_4$ and concentrated in a rotary evaporator and weighed. Yield = 2.38 g; 85%.

Preparation of 5-butyl-2-thiophenedithiocarboxylic acid ($C_4H_9TCS_2H$)

In the second step 2-butyl thiophene was converted into 5-butyl-2-thiophenedithiocarboxylic acid. The first part of the reaction was done in an inert atmosphere. n-Butyl lithium (12.5 ml, 20.0 mmol) was added to a solution of THF (50.0ml) and hexane (30.0 ml), which was cooled to -20°C. 2-Butyl thiophene (2.38 g, 17.0 mmol) was introduced over 10 minutes with cooling between 0°C and 10°C. The cooling bath was removed and allowed to rise to room temperature and stirred for a further 10 minutes. The solution was cooled to 0°C and copper(I) bromide (0.1 g) was added. Carbon disufide (1.29 g, 17.0 mmol) was added drop-wise to the stirred mixture. The colour of the reaction mixture changed to a deep-red colour. The cooling bath was removed and allowed to rise to the room temperature and stirring was continued for a further 1 hour. Ice water (100.0ml) was added followed by dilute hydrochloric acid (20.0 ml, 1mol/dm^3). The next part was done in air. The organic layer was separated and

extracted into diethyl ether (70.0 ml) and washed with 2 x 50.0 ml of water. The product was dried over $MgSO_4$ and the solvent removed in *vacuo*. Yield = 3.30 g; 89.8%.

Preparation of sodium-5-butyl-2-thiophenedithiocarboxylate ($C_4H_9TCS_2Na$)

The reaction was done in an inert atmosphere. Sodium metal (0.35 g, 15.28 mmol) was added over 10 minutes to vigorously stirred methanol (50.0 ml). When all the sodium had dissolved, additional (20.0 ml) methanol was added. 5-Butyl-2-thiophenedithiocarboxylic acid (3.30 g, 15.28 mmol) was added over 5 minutes to the mixture and left stirring for 30 minutes. The solvent was removed *in vacuo*, leaving the sodium 5-butyl-2-thiophenedithiocarboxylate as an orange-brown solid. Yield = 3.09 g; 85%.

Synthesis of bis(5-butyl-2-thiophenedithiocarboxylato)zinc(II) [$Zn_2(S_2CTC_4H_9)_4$]

The procedure was similar to that of Adams *et al*[4], who prepared dithiobenzoate complexes. The reaction was done in air. To a stirred solution of sodium 5-butyl-2-thiophenedithiocarboxylate (1.55 g, 6.5 mmol) in water (25.0 ml) was added drop-wise a colourless solution of $ZnCl_2$ (0.41 g, 3.0 mmol) in water (10.0 ml) at room temperature. The colour of the solution turned orange-brown and the mixture was left to stir for 3 hours. The mixture was concentrated to 25.0 ml on a rotary evaporator and 20.0 ml of methanol was added. The precipitate was separated by filtration and dried. The product was an oily solid. The product was purified on a silica gel column with hexane as the initial eluent and the first and second fraction on evaporations obtained as an oily red liquid. The desired

product was eluted from the column with hexane:CH_2Cl_2 (1:1). An orange powder was obtained on evaporation of the solvent. Yield = 0.49 g, 33%.

Five complexes of the type bis(5-alkyl-2-thiophenedithiocarboxylato)zinc(II) were synthesized by varying the alkyl chain, C_4H_9, C_6H_{13}, C_8H_{17}, $C_{12}H_{25}$ and $C_{16}H_{33}$. All the complexes were isolated as solids. The experimental results of complexes **7-11** are given in Table 3.5.

Table 3.5 Experimental results of **7-11** complexes

Complex	Colour	Mass (g)	Yield (%)
7	Orange	0.49	33
8	Orange	0.76	46
9	Reddish-orange	0.79	52
10	Dark orange	0.82	38
11	Dark orange	0.79	32

3.4 Conclusion

The reactions of a series of 5-alkyl-2-thiophenedithiocarboxylates with zinc(II) chloride formed zinc(II) complexes with terminal dithiocarboxylate ligands. The colour of the products is orange or dark orange. The zinc complexes are less soluble than the nickel analogues. A X-ray structure determination of complex **8** showed it to be dimeric, containing 8-membered $Zn_2S_4C_2$ rings, formed by the fusion of two ZnS_2C rings, and in which the geometry of sulfur about zinc approximated to trigonal bipyramidal with Zn-S intermolecular bond distance of

2.39 Å, being of the same order as Zn-S intramolecular bond distance of 2.33 – 2.77 Å. The X-ray structure is similar to the one for zinc bis[4-alkyloxy)dithiobenzoates described by Adams *et al.*[4]. Zinc alkyloxydithiobenzoate complexes are rod-shaped whereas the zinc thiophenedithiocarboxylate complex, **8** displays a step in its rod shape. Complexes **7-11** did not show any mesomorphic properties whereas zinc bis alkyloxy dithiobenzoates are reported to be mesomorphic[3]. It was reported that the dimeric structure persisted into the mesophase for the alkyloxydithiobenzoate complexes. The X-ray crystal structure of **8** showed that the distance between the zinc and the axial bridging sulfur, S(4)#1, is greater than in the zinc bis alkyloxy dithiobenzoates. Only EXAFS studies can confirm whether the dimeric structure retained during the melting process of **9** and **10.** It was reported that if the molecular forces are too strong, or if they are too weak, no mesophases will appear even if the molecular geometry is favourable for liquid crystalline properties[3]. Complexes **9** and **10** did not have liquid crystalline properties.

REFERENCES

1. P. A. Cotton and G. Wilkinson, *Advanced Inorganic Chemistry,* Fifth edition, John Wiley & sons Inc., **1988**, 608.
2. M. Bonamico, G. Dessy, V. Fares and L. Scaramuzza, *J. Chem. Soc., Dalton Trans*., **1972**, 2515.
3. H. Adams, N. A. Bailey, D. W. Bruce, R. Dhillon, D. A. Dunmur, S. E. Hunt, E. Lalinde, A. A. Maggs, R. Orr, P. Styring, M. S. Wragg and P. M. Maitlis, *Polyhedron*, **1988**, 7, 1861.
4. H. Adams, A. C. Albeniz, N. A. Bailey, D. W. Bruce, A. S. Cherodian, R. Dhillon, D. A. Dunmur, P. Espinet, J. L. Feijoo, E. Lalinde, P. M. Maitlis, R. M. Richardson and G. Ungar, *J. Mater. Chem*., **1991**, 1, 843.
5. A-M. Giroud-Godquin and P. M. Maitlis, *Angew. Chem., Int. Ed. Engl*., **1991**, 30, 375.
6. E. Terazzi, J.-M. Benech, J.-P. Rivera, G. Bernardinelli, B. Donnio, D. Guillon and C. Piguet, *J. Chem. Soc., Dalton Trans*., **2001**, 769.
7. B. A. Gregg, M. A. Fox and A. J. Bard, *J. Chem. Soc., Chem. Commun*., **1987**, 1134.
8. D. Guillon, A. Skoulios, C. Piechocki, J. Simon and P. Weber, *Mol. Cryst., Liq. Cryst*., **1983**, 100, 275.
9. L. M. Severs, A. E. Underhill, D. Edwards, P. Wight and D. Thetford, *Mol. Cryst., Liq. Cryst*., **1993**, 234.
10. J. Sleven, T. Cardinaels, C. Gorller-Walrand and K. Binnemans, *ARKIVOC*, **2003** (iv) 68.

11. K. Ohta, G. J. Jiang, M. Yokoyama, S. Kusabayashi and H. Mikawa, *Mol. Cryst., Liq. Cryst*., **1981**, 66, 283.

12. D. W. Bruce, D. A. Dunmur, L. S. Santa and M. A. Wali, *J. Mater. Chem*., **1992**, 2, 363.

13. N. Hoshino, R. Hayakawa, T. Shibuya and Y. Matsunaga, *Inorg. Chem*., **1990**, 29, 5129.

14. Q. M. Wang and D. W. Bruce, *Tetrahedron Letters*, **1996**, 37, 7641.

15. R. Gimenez, A. B. Manrique, S. Uriel, J. Barbera and J. L. Serrano, *Chem. Commun*., **2004**, 2064.

16. G. Barberio, A. Bellusci, A. Crispini, M. Ghedini, A. Golemme, P. Prus and D. Pucci, *Eur. J. Inorg. Chem.*, **2005**, 181.

17. W. Date, E. Fernandez Iglesias, K. E. Rowe, J. M. Elliott and D. W. Bruce, *Dalton Trans*., **2003**, 1914.

18. L. Brandsma and H. D. Verkruijsse, *Preparative Polar Organometallic Chemistry, Volume 1*, Springer Verlag, Heidelberg, **1987**, 124.

19. M. L. Shankaranarayana and C. C. Patel, *Can. J. Chem*., **1961**, 39, 1633.

20. J. M. Burke and J. P. Fackler (jr), *Inorg. Chem.*, **1972**, 11, 3000.

21. L. J. Farrugia, *J. Appl. Crystallogr*., **1997**, 30, 565.

22. The POV-Ray Team, POV-Ray 2004, URL: http://www.pov-ray.org./download/.

23. S. A. Cooke, J. H. Holloway and A. C. Legon, *Chem. Phys. Lett.*, **1998**, 298, 151.

24. K. Ohta, A. Ishii, H. Muroki, I. Yamamoto and K. Matsuzaki, *Mol. Cryst., Liq. Cryst.,* **1985**, 116, 299.

25. T. Seshadri and H. –J. Haupt, *J. Mater. Chem*. **1998.**, 8, 1345.

26. L. Jongen, K. Binnemans, D. Hinz and G. Meyer, *Mater. Sci Eng.*, **2001**, C18, 199.

27. G. H. Spies and R. J. Angelici, *Organometallics*, **1987**, 6, 1902.